Journal of proteome research

pubs.acs.org/jpr

Article

Genome Sequence, Proteome Profile, and Identification of a Multiprotein Reductive Dehalogenase Complex in *Dehalogenimonas alkenigignens* Strain BRE15M

Alba Trueba-Santiso,[⊥] Kenneth Wasmund,[⊥] Jesica M. Soder-Walz, Ernest Marco-Urrea,* and Lorenz Adrian

Cite This: *J. Proteome Res.* 2021, 20, 613−623

Read Online

ACCESS | Metrics & More | Article Recommendations | Supporting Information

ABSTRACT: Bacteria of the genus *Dehalogenimonas* respire with vicinally halogenated alkanes via dihaloelimination. We aimed to describe involved proteins and their supermolecular organization. Metagenomic sequencing of a *Dehalogenimonas*-containing culture resulted in a 1.65 Mbp draft genome of *Dehalogenimonas alkenigignens* strain BRE15M. It contained 31 full-length reductive dehalogenase homologous genes (*rdhA*), but only eight had cognate *rdhB* gene coding for membrane-anchoring proteins. Shotgun proteomics of cells grown with 1,2-dichloropropane as an electron acceptor identified 1152 proteins representing more than 60% of the total proteome. Ten RdhA proteins were detected, including a DcpA ortholog, which was the strongest expressed RdhA. Blue native gel electrophoresis (BNE) demonstrating maximum activity was localized in a protein complex of 146−242 kDa. Protein mass spectrometry revealed the presence of DcpA, its membrane-anchoring protein DcpB, two hydrogen uptake hydrogenase subunits (HupL and HupS), an iron−sulfur protein (HupX), and subunits of a redox protein with a molybdopterin-binding motif (OmeA and OmeB) in the complex. BNE after protein solubilization with different detergent concentrations revealed no evidence for an interaction between the putative respiratory electron input module (HupLS) and the OmeA/OmeB/HupX module. All detected RdhAs comigrated with the organohalide respiration complex. Based on genomic and proteomic analysis, we propose quinone-independent respiration in *Dehalogenimonas*.

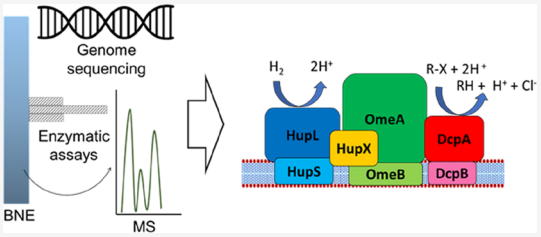

KEYWORDS: *organohalide respiration, dihaloelimination, Dehalogenimonas alkenigignens strain BRE15M, Dehalococcoidia, genome sequencing, 1,2-dichloropropane, proteome profiling*

INTRODUCTION

Organohalides are common soil and groundwater pollutants. Although they can be naturally produced, the high concentrations found at many industrial sites are due to improper storage or disposal practices and represent a threat to human and environmental health because of the toxicity or carcinogenicity of many of them.[1] A potential solution to treat sites impacted with organohalides relies on organohalide-respiring bacteria (OHRB), which can use organohalides as electron acceptors to harness energy and the reduction often results in decreased toxicity of the contaminants.[2]

Reductive dehalogenation is catalyzed by enzymes termed reductive dehalogenases (RDases). Respiratory RDases in OHRB have conserved features in their amino acid sequence including a twin arginine translocation (TAT)-leader peptide that tags the protein for transport to and/or across the cytoplasmic membrane, and two iron−sulfur cluster binding motifs.[3] Almost all characterized RDases contain a corrinoid in the active center, although corrinoid-binding motifs have seldom been found in the amino acid sequences.[4] Typically, RDases are encoded in operons composed by at least two genes: *rdhA*, encoding for the catalytically active subunit RdhA, and *rdhB* encoding a putative membrane anchor RdhB.[5] RdhA proteins are usually located attached to the cytoplasmic membrane facing the outer surface, indicating the need for both, the TAT-leader peptide and the putative membrane-anchoring RdhB protein.

In many OHRB, quinones play an important role as electron carrier between electron supplying protein complexes and the RDase (e.g., in *Sulfurospirillum* or *Dehalobacter*).[6] In these cases, energy is conserved via the quinone-mediated transport of protons across the membrane.[6] In contrast, the genomes of the obligate OHRB *Dehalococcoides* spp. lack the genes for complete biosynthesis of quinones.[6−8] In quinone-independent reductive dehalogenation, energy conservation was suggested

Received: July 23, 2020
Published: September 25, 2020

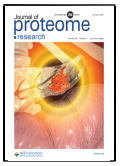

https://dx.doi.org/10.1021/acs.jproteome.0c00569
J. Proteome Res. 2021, 20, 613−623

to be coupled to the transfer of electrons from a hydrogenase to a complex iron−sulfur molybdoenzyme (CISM).[9] Recent studies have described a quinone-independent respiratory chain in *Dehalococcoides mccartyi* strain CBDB1, catalyzed by an organohalide respiration complex (OHR complex) that directly transfers the electrons derived from H_2 oxidation by hydrogen uptake hydrogenase (Hup) via a CISM to the RDase.[10] In this proposed scheme, Fe−S clusters in several of the multiprotein complex subunits act as an electron relay between hydrogenase and RDase.[9,11] According to Seidel et al.,[11] the new nomenclature OmeA/OmeB was proposed for the CISM α- and γ-subunit, standing for organohalide respiration-involved molybdoenzyme. HupX, encoded in the *hup* operon in *Dehalococcoides*, interacted strongly with OmeA and OmeB, forming a tight module. A much less strong interaction was found between the OmeA/OmeB/HupX module and a hydrogenase module HupS/HupL.

Bacteria of the genus *Dehalogenimonas* are obligate OHRB (class Dehalococcoidia), and were known for their potential to use vicinally halogenated alkanes.[12] Recently, isolated *Dehalogenimonas* strains have been shown to also respire with chlorinated ethenes and benzenes.[13,14] To date, the genomes of five *Dehalogenimonas* strains have been sequenced: (i) *Dehalogenimonas lykanthroporepellens* strain BL-DC-9^T,[15] (ii) *Dehalogenimonas alkenigignens* strain IP3-3,[16] (iii) *Dehalogenimonas* strain WBC-2,[17] (iv) *Dehalogenimonas formicexedens* strain NSZ-14T,[18] and (v) "Candidatus *Dehalogenimonas etheniformans*" strain GP.[13] Only three proteins involved in organochlorine respiration have been characterized in *Dehalogenimonas* spp.: (i) DcpA has been shown to dechlorinate 1,2-dichloropropane (1,2-DCP) to propene,[19] (ii) TdrA was responsible for the hydrogenolysis of *trans*-dichloroethene to vinyl chloride,[17] and more recently, (iii) CerA was shown to catalyze the dechlorination of vinyl chloride to ethene.[13] The sequenced *Dehalogenimonas* genomes harbor 22−52 *rdhA* genes, and in contrast to all other known OHRB, most of them lack colocated genes for membrane-anchoring protein cognates (*rdhB*), a feature that remains unexplained.

Previous work in our laboratory focused on enriching a nonmethanogenic *Dehalogenimonas*-containing culture from sediment samples collected from the Besòs River estuary (Sant Adrià de Besòs, Barcelona, Spain), which appeared to exclusively transform vicinally halogenated alkanes via dihaloelimination.[20] The compounds transformed included 1,2-DCP, 1,2,3-trichloropropane, 1,2-dichloroethane, 1,1,2-trichloroethane, 1,1,2,2-tetrachloroethane, and 1,2-dibromoethane.[20−23] Here, we provide biochemical data on the molecular organization of the proteins involved in the respiratory chain of this novel *Dehalogenimonas* strain. For this, we obtained a high-quality draft genome sequence of strain BRE15M and applied a combination of proteome profiling, blue native polyacrylamide gel electrophoresis (BNE), dehalogenation activity assays and protein mass spectrometry. In line with recent studies with *D. mccartyi* strain CBDB1, our data suggest the existence of a quinone-independent respiratory dehalogenase protein complex in *Dehalogenimonas*, thereby extending the phylogenetic occurrence of these complexes outside of the genus *Dehalococcoides*.

MATERIALS AND METHODS

Cultivation of the *Dehalogenimonas*-Containing Culture

A *Dehalogenimonas*-containing sediment-free culture transforming 1,2-DCP to propene was maintained for more than 5 years in our laboratory as described elsewhere.[20] Each microcosm contained 70 mL of an anaerobic bicarbonate-buffered medium, reduced with $Na_2S{\cdot}9H_2O$ and L-cysteine (0.2 mM each), amended with 5 mM sodium acetate as carbon source, and gassed with N_2/CO_2 (4:1, v/v, 0.2 bar overpressure) and H_2 (added to an overpressure of 0.4 bar). All microcosms were cultivated under static conditions in the dark at 25 °C. To enrich the *Dehalogenimonas* population, we followed a dilution-to-extinction procedure[24] together with the addition of streptomycin (50 mg L^{-1}) and vancomycin (5 mg L^{-1}). Cultures were transferred into a fresh medium with an inoculum of 10% (v/v) after the dechlorination of two to three doses (100−500 μM) of 1,2-DCP.

For genome sequencing, 420 mL of this anaerobic enriched culture was used growing on 1,2-DCP as the only halogenated electron acceptor for 34 transfers (10% v/v). For proteomic studies, cultures growing on 1,2-DCP for >42 transfers (10% v/v) were used after the dechlorination of at least 2 mM 1,2-DCP.

Gas Chromatographic Analysis

1,2-DCP and propene were analyzed from headspace samples with a gas chromatograph (GC) model 6890N (Agilent Technologies; Santa Clara, USA) equipped with an HP-5 column (30 m × 0.32 mm with 0.25 μm film thickness; Agilent Technologies) and a flame ionization detector. Helium was used as the carrier gas (1.5 mL min^{-1}). The injector and detector temperatures were both set at 250 °C. After the injection of the sample (split ratio = 2:1), the initial oven temperature (40 °C), ramped at 10 °C min^{-1} to 50 °C, and then ramped at 20 °C min^{-1} to 120 °C. Both compounds were identified and quantified using external chemical standards. Nominal concentrations of 1,2-DCP and propene are expressed as μmol per L of liquid volume or in nanomoles per bottle or vial.

Metagenomic Sequencing and Genomic Analysis

Details regarding cell harvesting, DNA extraction, genome sequencing, and assembling are provided in the Supporting Information Materials and Methods section. A final automatic annotation was performed using the MicroScope annotation pipeline.[25] Locus numbers used in this article are derived from the MicroScope annotation. The locus numbers are prefixed with "BRE15M_v1_" and an accompanying number, whereby the first two digits denote the scaffold number, and the last four digits denote the gene number of each particular scaffold. Predicted proteins were searched for signal peptides mediating the export from the cytoplasm using SignalP-5.0.[26] Transmembrane helices were detected using TMHMM server.[27] Subcellular location predictions were performed using PSORTb server.[28] The genome is available at GenBank under accession QEFQ00000000. The genome and annotations are also publicly accessible in the MicroScope platform (https://mage.genoscope.cns.fr/microscope/home/index.php, accession WGS BRE15M.1).

Protein Profiling

For cell harvesting, triplicate 140 mL samples of a 1,2-DCP dechlorinating *Dehalogenimonas* culture were separately centrifuged at 8000*g* and 10 °C to a final volume of 1 mL. A

https://dx.doi.org/10.1021/acs.jproteome.0c00569
J. Proteome Res. 2021, 20, 613−623

detailed protocol is provided in the Supporting Information Materials and Methods section. Cells were lyzed by freeze−thawing (−20 °C/+20 °C, 6×) and sonication for 30 s. The samples were then concentrated by ultrafiltration with Amicon Ultra 0.5 mL centrifugal filter units with a 10 kDa cutoff (Millipore) at 14,000*g* for 30 min at 10 °C. After centrifugation, filters were turned upside down and the protein extract was spun off for 2 min at 1000*g*, 10 °C. Protein concentrations in the obtained samples were quantified by the Bradford method. All triplicate samples were then processed by in-solution digestions for nano-liquid chromatography tandem mass spectrometry (nLC−MS/MS) as described below.

Blue Native Gel Electrophoresis

For each BNE gel, 140 mL samples of a 1,2-DCP dechlorinating *Dehalogenimonas* culture were centrifuged as described above. One milliliter of aliquoted concentrated cells was centrifuged again at 9000*g* for 20 min and 800 μL of the supernatant was removed. Then, 1× PBS buffer (pH 7.2) was added to a final volume of 600 μL. Cell density was quantified at this point by direct epifluorescence microscopic cell counting on slides covered with agarose as previously described.[29] Then, cells were lysed by a bead beater (FastPrep FP120, Thermo) at speed 4 m s^{-1}, in six cycles of 40 s beating alternated with 1 min resting in ice. Membrane proteins were solubilized by adding *n*-dodecyl β-D-maltoside (DDM) to a concentration of 0.05, 0.1, or 1% w/v, and incubating the samples at 10 °C for 1 h with gentle shaking under anaerobic conditions. After DDM incubation, samples were centrifuged at 16,600*g* for 45 min at 4 °C. The supernatant (DDM-solubilized protein extract) was amended with 0.125% w/v Coomassie G-250 additive and loaded in triplicate wells (25 μL/well) onto a precasted 4−16% gradient Bis-Tris gel (NativePAGE Novex, Invitrogen) and run inside an anaerobic glove box, maintaining the BNE system in contact with ice packs. Light blue cathode buffer and anode buffer were prepared following the manufacturer's instructions, degassed, and cooled down to 4 °C before the electrophoresis was started. NativeMark Unstained Protein Standard (Invitrogen) was used as protein ladder. Electrophoresis was run at 150 V for 60 min, and then at 200 V for 30 min more. Once the electrophoresis was finished, one of the replicate lanes and the protein ladder lane were cut from the gel using a scalpel and the protein bands were stained for visualization by a short silver staining method.[30] The rest of the gel was stored in anode buffer at 4 °C.

Dehalogenase Activity Assays

To test RDase enzyme activity, specific assays were set-up inside an anoxic glove box.[31] Anoxic 10 mL glass vials were used, containing 2 mL of an assay buffer with 200 mM potassium acetate buffer (pH 5.8), 2 mM methyl viologen, and 2 mM titanium(III) citrate [2 mM in respect to titanium(III)] and amended with 200 μM of 1,2-DCP. For the whole-cell activity assays, 200 μL of a cell concentrate (10^9 to 10^{10} cells mL^{-1}) were inoculated to each assay vial. These experiments were performed in triplicates.

To measure activity in BNE gels, a nonstained lane from the BNE was cut into slices using a steel scalpel. Each slice was introduced into a 2 mL assay vial. Slices were smashed into smaller pieces to better expose proteins to the assay buffer. The vials were closed with Teflon-coated rubber septa and aluminum crimps and amended with 1,2-DCP from a 1 mM acetone stock solution with a glass syringe (Hamilton) to a final concentration of 200 μM 1,2-DCP.

For each activity measurement from BNE gels, different controls were included. As a positive control, 25 μL of the crude protein extract were added to the assay buffer instead of a slice. Also, controls with either 25 μL supernatant of the solubilized protein extract or the remaining pellet after solubilization were included to evaluate the efficiency of the membrane protein extraction. To control for abiotic transformation of 1,2-DCP, parallel negative controls containing the assay buffer (i) without cells or gel slices from outside the area where proteins were loaded and (ii) with 25 μL of crude extract but no 1,2-DCP was included to test the production of propene from other sources than 1,2-DCP. All controls were performed in triplicate.

The activity test vials were thoroughly mixed and incubated upside down inside the glove box, at 30 °C without shaking. After 24 h, the headspace of each sample was analyzed for propene production by gas chromatography.

Protein Identification

Silver stained bands were cut from BNE gels, the bands were washed with ddH_2O and destained in a 1:1 (v/v) mixture of 30 mM $K_3[Fe(CN)_6]$ and 100 mM $Na_2O_3S_2$. Destained BNE bands and in-solution samples were treated as described previously to reduce and alkylate cysteine residues.[11] Protein digestion from both in gel and in-solution samples was done overnight at 37 °C on a shaker after the addition of 0.1 μg of porcine trypsin (Proteomics Sequencing Grade, Promega). The obtained peptides were extracted from the slices by 10 min incubation in a solution containing formic acid 5% (v/v) and acetonitrile 50% (v/v) three times and afterward extracts were combined. Extracts from both in gel and in-solution samples were dried, resolubilized in 0.1% of formic acid solution, and desalted using ZipTip-μC18 material (Merck Millipore).

Peptides were analyzed by nLC−MS/MS on a nanoUPLC system (nanoAcquity, Waters) hyphenated via a TriVersa NanoMate (Advion, Ltd., Harlow, UK) to an Orbitrap Fusion mass spectrometer (Thermo Scientific) as described previously.[11] Glyceraldehyde-3-phosphate dehydrogenase from *Staphylococcus aureus* was used as internal standard and was added to the gel slices before derivatization.

Peptide identification was conducted by Proteome Discoverer (v2.2, Thermo Fisher Scientific) using SequestHT as a search engine and a FASTA-file of proteins from the draft genome of the *Dehalogenimonas* strain in the culture as a database. False discovery rates for peptide identification of 1% was set as threshold, calculated versus a decoy database using the percolator node. Label free quantification of the detected proteins was performed with the abundance value obtained from Proteome Discoverer Minora node. The relative protein abundance in this study was defined as the abundance of a protein in one slice relative to the total abundance of this protein across all slices of the BNE gel lane. To detect the selenocysteine residue in OmeA different versions of the protein with a selenocysteine, a cysteine, or a serine instead of the TGA stop codon were added to the database and the search algorithm was adapted to detect selenocysteine as a modification of cysteine. Results were confirmed by manually examining the respective MS2 spectra.

https://dx.doi.org/10.1021/acs.jproteome.0c00569
J. Proteome Res. 2021, 20, 613−623

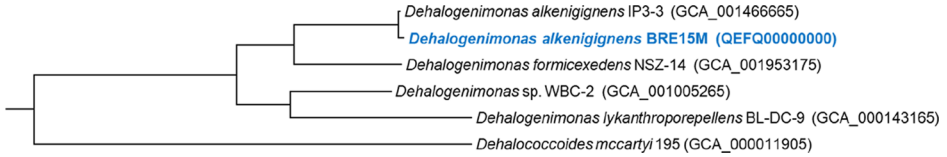

Figure 1. Phylogenetic tree showing the relationship of *D. alkenigignens* strain BRE15M to other strains of *Dehalogenimonas* and *D. mccartyi* strain 195 using a phylogenomic approach. Phylogenetic analysis was performed using an alignment of concatenated protein sequences of 34 single copy marker genes from CheckM analyses.[32] The tree was constructed using default parameters using FastTree (version 2.1.10).[33] The scale bar represents 5% sequence divergence. GenBank accession numbers are in parentheses.

Table 1. List of RdhA Proteins Detected in Full Protein Extracts of *D. alkenigignens* Strain BRE15M Grown with 1,2-DCP as Only Halogenated Substrate for More Than 35 Transfers[a]

	replicate 1		replicate 2		replicate 3	
accession	abundance	rank	abundance	rank	abundance	rank
BRE15M_v1_160008 (DcpA)	7.34×10^7	88	2.40×10^8	10	3.44×10^8	7
BRE15M_vl_160007	4.55×10^7	134	7.95×10^7	41	1.32×10^8	30
BRE15M_v1_40117	3.46×10^7	162			1.19×10^7	375
BRE15M_v1_30017	2.17×10^7	246	1.27×10^7	276	1.77×10^7	300
BRE15M_v1_10074			5.44×10^6	435	1.32×10^7	348
BRE15M_v1_150026	6.46×10^5	808	2.51×10^6	583	2.99×10^6	654
BRE15M_v1_30093	1.11×10^6	724				
BRE15M_v1_30016	2.48×10^6	622	5.84×10^5	823	1.34×10^5	1086
BRE15M_v1_30086	1.22×10^5	896	9.75×10^4	940	1.82×10^6	746
BRE15M_v1_170013					9.49×10^4	1100
protein concentration in the sample in mg/mL	6.9		2.14		5.08	
number of detected proteins	901		947		1114	
sum of abundances of all detected proteins	2.74×10^{10}		1.84×10^{10}		2.61×10^{10}	

[a]The rank columns show the rank of a protein relative to all proteins in that sample, calculated from the abundance values. Empty cells indicate that a protein was not detected in this replicate.

RESULTS

Draft Genome Sequence of *D. alkenigignens* BRE15M

Metagenome sequencing was performed on DNA extracted from the enrichment culture to investigate the genomic properties of the *Dehalogenimonas* strain and to allow for further proteomic studies. A high-quality draft genome of a *Dehalogenimonas* sp. was obtained consisting of a total of 1,654,503 bp within 18 contigs, a GC content of 56.3%, and containing 1795 predicted protein coding genes, all similar to reported *Dehalogenimonas* genomes (Table S1). CheckM results indicated that the genome was 97.8% complete with no contamination (0%).[32] In line with previous 16S ribosomal RNA (rRNA) gene sequencing of cultures from this enrichment,[20] the 16S rRNA gene of the *Dehalogenimonas* genome was 100% identical to the 16S rRNA gene of *D. alkenigignens* strain IP3-3, suggesting the strain in our culture belongs to the species *D. alkenigignens*. Average nucleotide identity (gANI) of the whole genome to *D. alkenigignens* strain IP3-3 showed 98.7% ANIb (BLASTN) identities from approximately 92% of the regions that aligned. We denominated our strain *D. alkenigignens* strain BRE15M. The close similarity with *D. alkenigignens* was further supported by phylogenetic analysis of concatenated protein sequences derived single copy marker genes (Figure 1). Reciprocal BLASTP analyses of protein sequences from *D. alkenigignens* strains BRE15M and IP3-3 suggested no major functional differences exist between the strains (Supporting Information Results section).

The genome contains 31 full-length *rdhA* genes that were not truncated by contig breaks, while two additional partial *rdhA* (BRE15M_v1_070029 and BRE15M_v1_150066; in the following section the MicroScope gene locus tag "BRE15M_v1" will be omitted) were apparently truncated because of being at contig break. Only eight *rdhA* had cognate genes for membrane-anchoring proteins encoded directly adjacent to the *rdhA* (Table S2). In total, six *rdhB* were automatically predicted, and we manually identified three additional possible *rdhB* that were adjacent to *rdhA* and encoded proteins with transmembrane helixes that may anchor RdhA proteins into membranes (Table S3, Figure S1). Interestingly, one *rdhB* gene (_030121) was found at a locus where no *rdhA* was present, the closest being over 22 kbp away. This brought into question whether the encoded protein may be functional as an RdhB. We therefore searched for closest homologs of this protein in other Dehalococcoidia. Although the closest homologs to this RdhB in other *Dehalogenimonas* spp. were also not adjacently encoded to an *rdhA* gene, several homologs with >80% amino acid identity in multiple *D. mccartyi* strains (CBDB1, DCMB5 and VS) harbored an adjacently encoded RdhA. Together this suggests locus _030121 encodes a functional RdhB.

The genome encoded various uptake and cytoplasmic hydrogenases, formate dehydrogenases and a possible OHR complex, similar to previously described in *Dehalococcoides* spp.[9,11] No genes for biosynthesis of quinones or cytochromes were found. Further details regarding gene annotations and protein properties are presented in the Supporting Information Results section.

Proteome Profiling

The shotgun proteomic analysis of strain BRE15M grown with 1,2-DCP identified a total of 1152 proteins, which represented the 64% of the annotated proteins in strain BRE15M (Table

https://dx.doi.org/10.1021/acs.jproteome.0c00569
J. Proteome Res. 2021, 20, 613−623

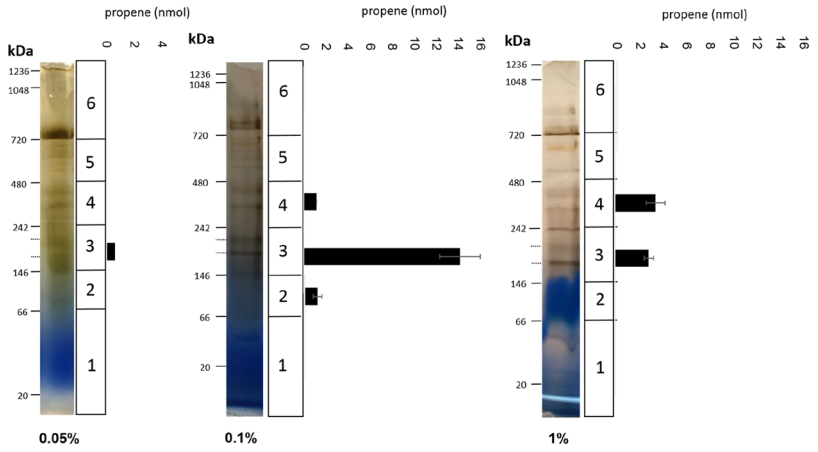

Figure 2. Distribution of dehalogenating activity in BNE with protein membrane samples of strain BRE15M solubilized with 0.05, 0.1 or 1% (w/v) DDM after lysis by bead beating. Dehalogenating activity was measured in nanomoles of propene produced from 1,2-DCP after 24 h of incubation. Data shows means of duplicate cultures ±SD. Dehalogenating activity in the corresponding controls is shown in Table S14.

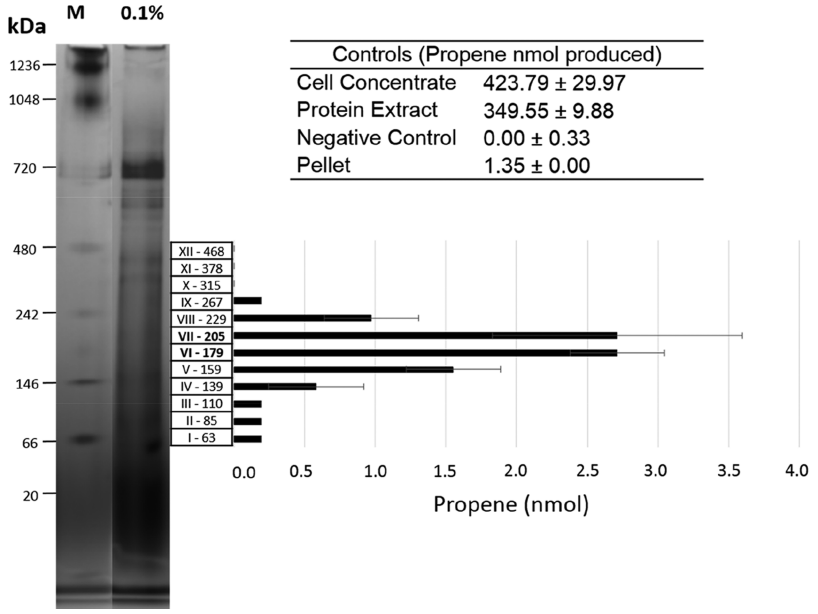

Figure 3. Distribution of dehalogenating activity in BNE with protein samples of strain BRE15M solubilized with 0.1% (w/v) DDM after lysis by bead beating. Dehalogenating activity was measured as nmol propene derived from 1,2-DCP dihaloelimination detected in enzyme assays within gel slices. Data shows means of duplicate culture samples ±SD. Molecular weight ranges were estimated from gel images using Image Lab software. "M": protein molecular mass marker.

S12). A total of 10 RDases were expressed in strain BRE15M when grown with 1,2-DCP (Tables 1 and S12). The most abundantly expressed RDase (_160008) was an ortholog of the RDase DcpA, which catalyzes reduction of 1,2-DCP to propene in *D. mccartyi*, *Dehalogenimonas* and uncultured bacteria. The RDase _160008 had >90% amino acid sequence identity to DcpA (Table S13).[19] The second most abundant RDase (_160007) is encoded adjacently to the DcpA ortholog and its putative membrane-anchoring protein DcpB (_160009) (Figure S2). Interestingly, _160007 is one of the four RDases which lacks the TAT signal peptide and has a predicted cytoplasmic location according to Phobius[34] (Table S2).

A membrane-bound [NiFe] hydrogenase (HupL/HupS, _070001, _070002), was expressed at high abundance (absolute abundance > 10^6) as described for *D. mccartyi* strains.[9,11,35] Also other proteins reported to be part of the OHR complex: OmeA (_040002/_040003), HupX (_040001) and OmeB (_130001)[9,11] were detected in each of the protein extract triplicates of strain BRE15M with >10^6 abundance. None of the few annotated genes involved in heme or quinone biosynthesis were expressed, further supporting the conclusion that strain BRE15M is independent from cytochromes and quinones. Finally, heterodisulfide reductase A and B subunits (_010277 and _010278) were expressed in strain BRE15M, proteins that are not encoded in *D. mccartyi* strains.[13]

Detection of the OHR Complex of Strain BRE15M by BNE

When membrane proteins of strain BRE15M were solubilized in 1% DDM without an additional cell disruption step and separated by BNE, dehalogenating activity was detected in gel slices corresponding to a molecular mass range between 146 and 242 kDa (Table S14). The activity produced low amounts of propene from 1,2-DCP by dichloroelimination. No defined

https://dx.doi.org/10.1021/acs.jproteome.0c00569
J. Proteome Res. 2021, 20, 613−623

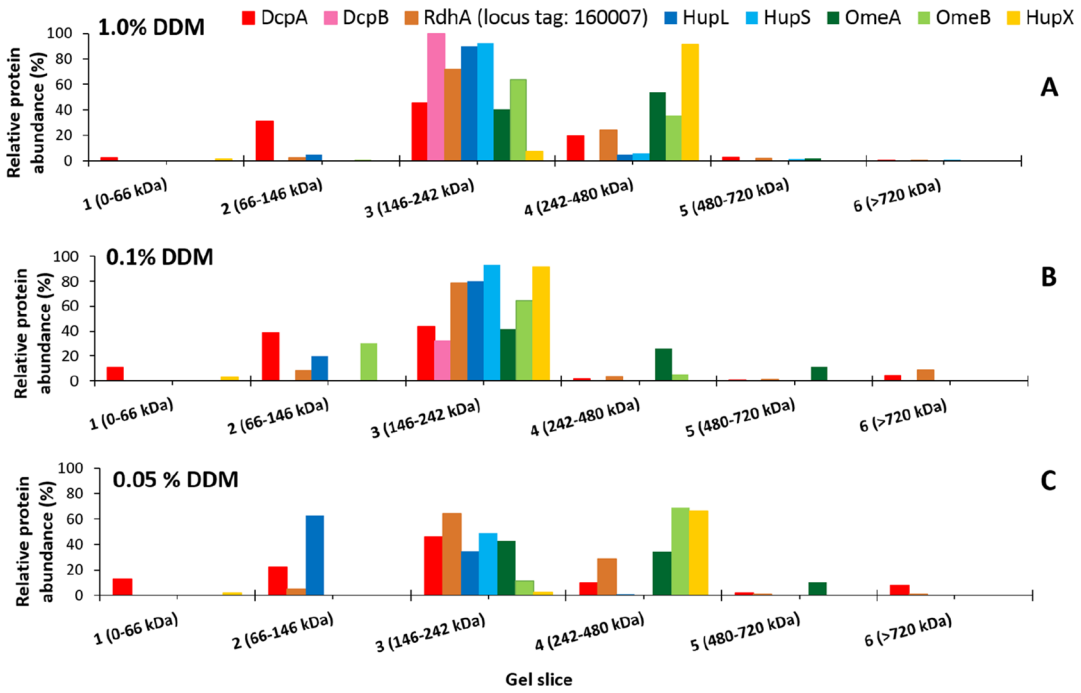

Figure 4. Relative abundance of proteins predicted to be associated with the OHR complex at different molecular weights in BNE gels after solubilization of strain BRE15M cells at different concentrations of DDM (panel A: 1% DDM, panel B: 0.1% DDM, panel C: 0.05% DDM).

bands were observed in the gel after silver staining (not shown), and most of the dehalogenating activity detected in the controls remained in the pellet control (390.14 ± 1.77 nmol propene), compared to the protein extract supernatant (146.93 ± 0.75 nmol propene). Together, this indicated inefficient protein extraction (Table S14).

Next, cell disruption by bead beating combined with solubilization with three different DDM concentrations was tested (0.05, 0.1 and 1% DDM). The detailed conditions for these experiments are shown in Table S15. The resolution of the protein bands in the native gel was different among the three conditions tested (Figure 2). With 0.05% DDM, the observed bands were very weak and blurry. On the contrary, in 1.0% DDM bands were defined and intense, however, the bottom part of the gel (lower molecular weight) repeatedly showed a blue Coomassie accumulation that impeded the visualization of the bands located below. With 0.1% DDM bands were well defined along the whole lane. Parallel unstained gel lanes with the three DDM concentrations were cut into six slices each, following the stained molecular mass ruler marks and each section was subjected to a dehalogenase enzyme activity test with 1,2-DCP as electron acceptor. Propene was detected in all gel slices corresponding to a molecular weight of 146−242 kDa in the three gel lanes. Activity was also detected in gel slices at 242−480 kDa in gels with 0.1 and 1% DDM, and at 66−146 kDa in the gel with 0.1% DDM (Figure 2). Overall, a slight shift of the reductive dehalogenation activity toward higher molecular weight fractions was observed at higher DDM concentration. Notably, maximum dehalogenating activity was detected in the molecular weight range between 146 and 242 kDa with 0.1% DDM (Figure 2). Dehalogenating activity was never detected below 66 kDa in any of the experiments, indicating that monomeric RdhA protein (~50 kDa) was part of a higher molecular mass respiratory complex or that it lost its activity as a monomeric enzyme.

To narrow down the molecular range of the maximum dehalogenating activity, two replicate gel lanes with 0.1% DDM were cut into slices of ~2 mm across the mass range of 63−490 kDa and were subjected to activity assays (Figure 3). Maximum activity was detected in slices VI and VII in both gels, corresponding to molecular weights of 179−229 kDa. These results strongly support the presence of a organohalide respiratory complex in strain BRE15M.

Mass Spectrometric Analysis of BNE Slices

Each of the six analyzed regions of the stained gels with 0.05, 0.1 and 1% DDM were subjected to in-gel trypsin digestion and subsequently analyzed by nLC−MS/MS. The number of unambiguously identified proteins for each gel region ranged from 175 to 966 (Figure S3). Thirteen RdhA paralogs were detected in the gel experiment treated with 0.05% DDM, 10 with 0.1% DDM and 9 with 1% DDM (Tables S16−S18). In accordance with the production of propene detected in the in-gel dehalogenating activity tests, the DcpA ortholog predicted to be involved in 1,2-DCP dihaloelimination was abundantly detected in gel regions from the molecular range 146−242 kDa (Figure S4). Interestingly, the RDase with locus tag _160007 was the most abundant RDase expressed in the slices with maximum dechlorinating activity in the gels with 0.1 and 0.05% (Figure S4).

In addition to RDases, we detected several other proteins in the gel slices in which the OHR complex was detected (full lists are given in Tables S16−S18). The DcpA ortholog and the RDase with the locus tag _160007 comigrated with the two hydrogenase subunits HupS and HupL, the OmeA, the putative membrane-integrated anchor OmeB, and the four-FeS cluster protein HupX, in gel regions that showed maximum in-gel dehalogenating activity (regions 3−4 in proteins solubilized with 1% DDM, and region 3 in proteins solubilized with 0.05 or 0.1% DDM) (Figures 2 and 4). These eight proteins showed a clear maximum of relative protein

https://dx.doi.org/10.1021/acs.jproteome.0c00569
J. Proteome Res. 2021, 20, 613−623

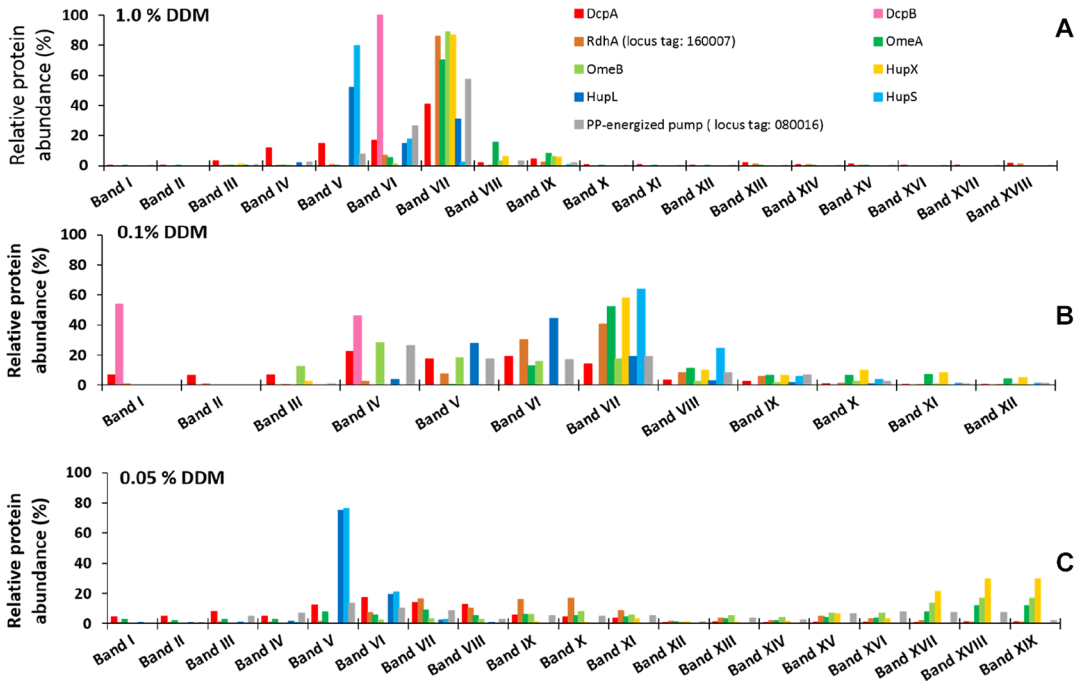

Figure 5. Relative abundance of proteins associated with the OHR complex at different molecular weights in BNE gels after solubilization of strain BRE15M cells at 1% DDM (panel A), 0.1% DDM (panel B), and 0.05% DDM (panel C).

abundance in region 3 in the gel with 0.1% DDM-extracted proteins.

Only one RdhB protein was identified with a single peptide in 0.1 and 1% DDM BNE slices being colocalized with the DcpA ortholog (Figure 4A,B). This RdhB protein with the locus tag _160009 is encoded in the same operon as DcpA in strain BRE15M (Figure S2) and shares 88% sequence identity (*e*-value 3×10^{-40}) with the DcpB (locus tag Dehly_1525) in *D. lykanthroporepellens* strain BL-DC-9, predicted to function as a membrane anchor for DcpA. Interestingly, the topology of DcpB in strain BRE15M differs from the majority of the RdhB reported so far, with two predicted transmembrane regions instead of three (Figure S1). In summary, the identified proteins constitute the putative subunits of the OHR complex in strain BRE15M, and appear to functionally correspond with the subunits recently described for the OHR complex in *D. mccartyi* strain CBDB1.

After determining protein composition in broad gel bands, we also determined the presence of proteins within single defined bands (~2 mm). For that we ran a sample on a BNE gel with proteins solubilized with 1% DDM, stained the gel with a silver protocol and analyzed dominant protein bands by nLC−MS/MS (Figure S5A, Table S19). As shown in Figure 5A, the RDases (catalytic subunit DcpA, and the RDase with locus tag _160007), the OmeA, the membrane subunit OmeB and the membrane-associated protein HupX were detected in the band VII (242 kDa). The membrane anchor DcpB colocalized with DcpA in band VI (202 kDa). The HupLS complex had its maximum relative abundance in band V (176 kDa). To date, it is unknown how protons are pumped across the membrane in *D. mccartyi* strains, but Seidel et al. (2018)[11] found that a protein annotated as a K^+-insensitive pyrophosphate energized proton pump (HppA) colocalized with the OmeA/OmeB/HupX module across BNE gels in *D. mccartyi* strain CBDB1. Interestingly, we detected the homologous HppA protein (_080016) with a maximum of relative protein abundance in band VII (Figure 5A), which coincides with the OmeA/OmeB/HupX module. Potentially supporting this physical association, the *hppA* gene was encoded within the same gene neighborhood as the omeA and hupX genes in *Dehalogenimonas* strains BRE15M and IP3-3.

The same procedure was followed for dominant protein bands in a silver-stained gel lane with 0.1% DDM-solubilized proteins focusing on the region 66−480 kDa (Figure S5B). All of the proteins suspected to be part of the respiratory complex were detected in band VII (205−229 kDa) with the exception of DcpB, and in band VI (179−205 kDa) with the exception of DcpB and HupS (Figure 5B, Table S20). These bands VI and VII corresponded to the unstained parallel gel slices with highest dehalogenating activity (Figure 3). HupL had its maximum of relative protein abundance in band VI (179 kDa), yet HupLS are detected together in band VII, which prevented the categorical assumption of an independent hydrogenase module. A remarkable observation was again the colocalization of the DcpB ortholog with its respective DcpA in band IV (139 kDa) in a region where HupX and OmeA were absent.

Finally, a BNE gel lane with proteins extracted with 0.05% DDM was analyzed (Figure S5C, Table S21). No RDase activity was detected in any of the 19 gel slices picked from the parallel unstained gel. All subunits of the complex described above, apart from DcpB, were again identified in the excised silver stained bands. However, the distribution of the relative protein abundance across the gel lane pointed to the presence of three modules (Figure 5C). The two subunits of the Hup complex exhibited identical migration patterns and shared a clear maximum relative abundance in band V (123 kDa) (Figure 5C), which coincides well with the predicted molecular weight of the dimer of HupL/HupS (93.9 kDa). This observation strengthens the hypothesis that HupL and HupS form a hydrogenase module also in *Dehalogenimonas* strains. The DcpA ortholog and the RdhA with locus tag _160007 had a similar migration pattern. Unlike the protein

https://dx.doi.org/10.1021/acs.jproteome.0c00569
J. Proteome Res. 2021, 20, 613−623

distribution observed in gels with the 1% DDM or 0.1% DDM solubilized proteins, both RdhA were found in all 19 slices, but never more than 20% of relative abundance. Similarly, the putative proton pump protein HppA was broadly distributed across the gel. As noted earlier, RdhB proteins were not detected from 0.05% DDM treatments, suggesting the need of a higher detergent concentration to detach this protein from membrane or from the complex. The OmeA/OmeB/HupX module reached its maximum of relative protein abundance in band XVIII (450−480 kDa), and they comigrated in the molecular range between 320 and 480 kDa (bands XV to XIX). This indicated that they were tightly connected to each other. Together, these results indicate weak interaction between the OmeA/OmeB/HupX module and the HupL/HupS module but strong interactions within the modules. The lack of dehalogenating activity in the different slices of this gel indicates the need of a full multimeric complex to proceed with organohalide respiration, rather than the RdhA catalytic subunit alone.

Based on these results, we propose a respiratory complex for strain BRE15M that includes subunits of the CISM complex, subunits of the Hup hydrogenase, and RDase subunits (Figure 6).

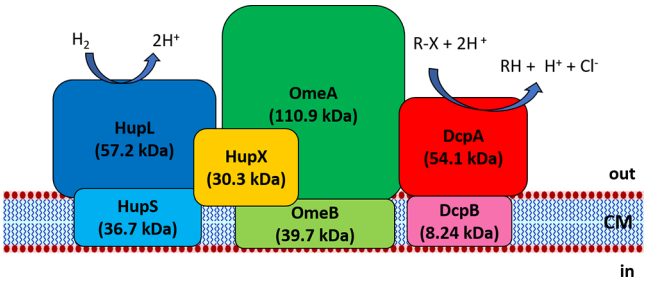

Figure 6. Model of the OHR complex of *D. alkenigignens* strain BRE15M. The proteins found throughout this study to be part of the suspected multimeric respiratory complex are the organohalide respiration involved molybdoenzyme OmeA (locus tag _040002/_040003), and its membrane-anchoring subunit OmeB (_130001), the hydrogenase large subunit HupL (_070001), and its small subunit HupS (_070002), the HupX (_040001), the RDase DcpA (_160008), and its putative membrane-anchor DcpB (_160009).

DISCUSSION

The draft genome sequence of strain BRE15M provides a basis to study its proteome profile and allowed for a characterization of its organohalide respiratory system. Annotation of the genome sequence excluded the possibility that organohalide respiration is quinone-mediated in *Dehalogenimonas* because no functional cytochromes or biosynthetic pathways for quinones were encoded. The genome encoded 31 full-length *rdhA*, 22 of which were detected in our proteomic experiments (Table S2), even though 1,2-DCP was the only halogenated electron acceptor in the medium. The two most abundant RdhA proteins (DcpA ortholog and _160007) are encoded together in one operon and were colocalized across the gels regardless of the DDM concentration. To date, DcpA was the only RdhA for which a 1,2-DCP dihaloelimination function was assigned.[19] However, in our study the RDase _160007 was detected at even higher abundances than DcpA in gels with proteins solubilized with 0.1 and 0.05% DDM (Figure S4). Further comparative proteomic studies with strain BRE15M growing with different electron acceptors can elucidate whether the RdhA _160007 is specifically induced by 1,2-DCP or, instead, whether its expression is either broadly induced or even constitutive. Constitutive expression of RdhA in OHRB is common, as illustrated by the dehalogenase CbdbA80 in *D. mccartyi* strain CBDB1.[36] The colocalization in the genome as well as in gel slices of these two RdhA may suggest either strong interaction, or that they are performing the same function in different copies of the respiratory complex. These results are nevertheless intriguing because RdhA _160007 does not have a TAT leader peptide. Further, no RdhA sequences from strain BRE15M contained predicted multiple transmembrane helix domains that might directly anchor them to membranes, as was recently described in other genomes.[37−39] One possibility is that both RDases are exported together as a heterodimer via the TAT machinery associated with the DcpA, and once in the outer part of the membrane, _160007 is either attached to a different copy of the DcpB or remains attached to DcpA forming a stable heterodimer in vivo. This hypothesis would assume that one RdhB protein can anchor different RdhA proteins to the membrane. If this is true, the four RdhA proteins without TAT leader peptide encoded in the genome might be anchored to one of the nine encoded RdhB, forming heterodimers with other RdhAs. This may occur even if the RdhA protein without TAT leader peptide is not encoded in the same operons as another RdhA protein. Alternatively, a feasible explanation for the lack of TAT leader peptide is that a RdhA protein might function as a cytoplasmatic nonrespiratory dehalogenase, as reported for aerobic bacteria[5,37] and that the association with the OHR complex is an artifact after cell disruption.

In this study, we also provide biochemical evidence that RDases in strain BRE15M are part of a large respiratory complex. The nonionic detergent DDM was suitable to detach membrane associated proteins while maintaining protein−protein interactions. Protein solubilization with 0.1% (w/v) DDM enabled the identification of a putative multiprotein complex composed by subunits of the CISM complex, a dimeric [NiFe] hydrogenase, and the RDase system in one single gel slice that was at a position in the gel with maximum dechlorination activity within the measured gel lane. Our results with lower DDM concentration (0.05%) were surprisingly counterintuitive because it led to partial disintegration of the protein complex. This might be explained by the fact that the ionic protein−protein interactions within the complex are not affected by this nonionic detergent, but they may disrupt lipid−protein interactions of membrane proteins. In contrast, increasing concentrations of DDM might drive the protein subunits to move together, as high salt pushes hydrophobic interaction together.

The analysis of the complexome using 0.05% (w/v) DDM, where the complex partially disintegrates, strongly suggests the presence of three modules. The largest module comprised OmeA, OmeB and HupX. The calculated size of this module of 180.9 kDa did not match with the molecular mass corresponding with the gel slice in which these proteins had its relative maximum abundance (band XVIII, Figure 5C, 450 kDa), suggesting that the Ome/HupX module polymerizes. As observed from the distribution of 0.05% DDM-solubilized proteins across the gel, HupX had a much stronger interaction with OmeA and OmeB than with the two hydrogenase subunits, which agrees with previous results with *D. mccartyi* strain CBDB1.[11] However, a noticeable difference between

https://dx.doi.org/10.1021/acs.jproteome.0c00569
J. Proteome Res. 2021, 20, 613−623

these two strains is that HupX is encoded in an operon together with HupL and HupS in *D. mccartyi* strain CBDB1,[10] while it forms an operon with OmeA and OmeB in strain BRE15M, further supporting its role as the four iron−sulfur cluster β-subunit of the CISM module. We also biochemically detected a protein annotated as K^+-insensitive pyrophosphate energized proton pump (HppA) that migrates similarly to the OmeA/OmeB/HupX module in a BNE gel with 0.1% DDM-solubilized proteins. However, the broad distribution of HppA across the bands in BNE gels with 0.05% DDM questions any strong interaction between HppA and the OmeA/OmeB/HupX module but provides a basis to speculate that HppA could be part of the respiratory complex of strain BRE15M and may translocate protons through the subunits of this complex.

The hydrogenase subunits HupL and HupS constitute another defined module and its facile separation from the other OHR complex subunits has also been observed in *D. mccartyi* strain CBDB1.[11] The molecular weight range in which the maximum relative protein abundance of these subunits was detected is 159−179 kDa in the 0.1% DDM treatment (band V) and 123−146 kDa in the 0.05% DDM treatment (band V), which slightly differs from the theoretical calculated size of 93.9 kDa for this module, however, size determinations in BNE gels can only considered as rough estimations. Finally, the RDase DcpA, which functioned as terminal reductase in the respiratory complex, is attached to the putative membrane anchor DcpB. We detected comigration of both proteins in BNE gels loaded with proteins solubilized with 1% DDM (band VI, 202 kDa, Figure 5A) and 0.1% DDM (band IV, 139 kDa, Figure 5B). These results constitute, together with a recent study with *D. mccartyi* strain CBDB1, one of the few biochemical evidences of specific interaction between an RdhA and its corresponding RdhB.[10]

■ ASSOCIATED CONTENT

Supporting Information

The Supporting Information is available free of charge at https://pubs.acs.org/doi/10.1021/acs.jproteome.0c00569.

Metagenomic sequencing and genomic analysis; cell harvesting protocol for 1,2-DCP-consuming *Dehalogenimonas* cultures; reciprocal BLASTP analyses of protein sequences from *D. alkenigignens* strains BRE15M and IP3-3; and draft genome annotation details: hydrogenases, formate dehydrogenases, possible organohalide respiratory complex, quinones, and cytochromes (PDF)

Genome data for *Dehalogenimonas* sequenced to date; list and characteristics of RdhAs encoded in the genome of strain BRE15M; characteristics of RdhBs encoded in the genome of strain BRE15M; ten best hits in BLASTp search against the amino acid sequence of the periplasmic [NiFeSe] hydrogenase large subunit from strain BRE15M; ten best hits in BLASTp search against the amino acid sequence of the periplasmic [NiFeSe] hydrogenase small subunit from strain BRE15M; ten best hits in BLASTp search against the amino acid sequence of the formate dehydrogenase, α subunit, from strain BRE15M; characteristics of the proteins identified in the multiprotein respiratory complex of strain BRE15M according to TMHMM server and PSORTb; ten best hits in BLASTp search against the amino acid sequence of the formate dehydrogenase two subunit α (cytochrome *c*-553) from strain BRE15M; ten best hits in BLASTp search against the amino acid sequence of the formate dehydrogenase β subunit from strain BRE15M; ten best hits in BLASTp search against the amino acid sequence of the protein automatically annotated as polysulfide reductase from strain BRE15M; ten best hits in BLASTp search against the amino acid sequence of the "protein of unknown function" (BRE15M_v1_040001) from strain BRE15M; protein concentration and total protein abundances of all of the proteins identified in triplicate samples of strain BRE15M; ten best hits in BLASTp search against the amino acid sequence of BRE15M_v1_160008 from strain BRE15M; propene production from 1,2-DCP after 24 h in enzymatic assays using slices of BNE gels; conditions of BNE experiments at different DDM concentrations; total protein abundances of all of the proteins identified in BNE gel slices after bead-beating and solubilization with 0.05%, 0.1%, and 1%; total protein abundances of all of the proteins identified in BNE dominant bands after bead-beating and solubilization with 0.1%, 0.05%, and 1%; prediction of transmembrane helices in putative RdhB protein in strain BRE15M; arrangement of the DcpA gene and the corresponding B gene, DcpB; number of proteins identified across the length of BNE gels cut into six regions after bead-beating and solubilization with different % of DDM; absolute abundance of RdhA proteins across the length of BNE gels cut into six regions after bead-beating and solubilization with different % of DDM; and silver-stained BNE gels with protein extracts after bead-beating and solubilization with different % of DDM (XLSX)

■ AUTHOR INFORMATION

Corresponding Author

Ernest Marco-Urrea − *Departament d'Enginyeria Química, Biològica i Ambiental, Universitat Autònoma de Barcelona (UAB), Bellaterra 08193, Spain;* orcid.org/0000-0002-8033-6553; Phone: +34 935812694; Email: ernest.marco@uab.es; Fax: +34935812013

Authors

Alba Trueba-Santiso − *Departament d'Enginyeria Química, Biològica i Ambiental, Universitat Autònoma de Barcelona (UAB), Bellaterra 08193, Spain*

Kenneth Wasmund − *Division of Microbial Ecology, Centre for Microbiology and Environmental Systems Science, University of Vienna, Vienna 1010, Austria*

Jesica M. Soder-Walz − *Departament d'Enginyeria Química, Biològica i Ambiental, Universitat Autònoma de Barcelona (UAB), Bellaterra 08193, Spain*

Lorenz Adrian − *Department of Environmental Biotechnology, Helmholtz Centre for Environmental Research—UFZ, Leipzig 04318, Germany; Chair of Geobiotechnology, Technische Universität Berlin, Berlin 10623, Germany;* orcid.org/0000-0001-8205-0842

Complete contact information is available at: https://pubs.acs.org/10.1021/acs.jproteome.0c00569

Author Contributions

⊥A.T.-S. and K.W. contributed equally to this work.

https://dx.doi.org/10.1021/acs.jproteome.0c00569
J. Proteome Res. 2021, 20, 613−623

Notes

The authors declare no competing financial interest.

■ ACKNOWLEDGMENTS

This work has been supported by the Spanish Ministry of Economy and Competitiveness State Research Agency (CTM2016-75587-C2-1-R and PID2019-103989RB-100) co-financed by the European Union through the European Regional Development Fund (ERDF). This work was partly supported by the Generalitat de Catalunya (Consolidate Research Group 2017-SGR-14). A.T.-S. acknowledges a predoctoral fellowship from the MINECO (BES-2014-070817) and a German Academic Exchange Service (DAAD) scholarship (pers. ref. no. 91726320). K.W. is supported by the Austrian Science Fund (FWF) grant no. P29246-B29. Protein mass spectrometry was done at the Centre for Chemical Microscopy (ProVIS) at the Helmholtz Centre for Environmental Research, which is supported by European regional development funds (EFRE−Europe Funds Saxony), and the Helmholtz Association. The work of L.A. was supported by the German Research Council (DFG) within the Research Group FOR1530 and the SPP1927. We thank the Biomedical Sequencing Facility (BSF) of Vienna, Austria, for DNA sequencing and support.

■ REFERENCES

(1) ATSDR. Priority List of Hazardous Substances. 2019, https://www.atsdr.cdc.gov/spl/index.html July 1 2020 .

(2) Blázquez-Pallí, N.; Rosell, M.; Varias, J.; Bosch, M.; Soler, A.; Vicent, T.; Marco-Urrea, E. Multi-method assessment of the intrinsic biodegradation potential of an aquifer contaminated with chlorinated ethenes at an industrial area in Barcelona (Spain). *Environ. Pollut.* **2019**, *244*, 165−173.

(3) Hug, L. A. Diversity, evolution, and environmental distribution of reductive dehalogenase genes. In *Organohalide-Respiring Bacteria*; Adrian, L., Löffler, F. E., Eds.; Springer Berlin Heidelberg: Berlin, 2016; pp 377−393.

(4) Hölscher, T.; Krajmalnik-Brown, R.; Ritalahti, K.; von Wintzingerode, F.; Görisch, H.; Löffler, F.; Adrian, L. Multiple nonidentical reductive-dehalogenase-homologous genes are common in *Dehalococcoides*. *Appl. Environ. Microbiol.* **2004**, *70*, 5290−5297.

(5) Chen, K.; Huang, L.; Xu, C.; Liu, X.; He, J.; Zinder, S. H.; Li, S.; Jiang, J. Molecular characterization of the enzymes involved in the degradation of a brominated aromatic herbicide. *Mol. Microbiol.* **2013**, *89*, 1121−1139.

(6) Schubert, T.; Adrian, L.; Sawers, R. G.; Diekert, G. Organohalide respiratory chains: composition, topology and key enzymes. *FEMS Microbiol. Ecol.* **2018**, *94*, fiy035.

(7) Schipp, C. J.; Marco-Urrea, E.; Kublik, A.; Seifert, J.; Adrian, L. Organic cofactors in the metabolism of *Dehalococcoides mccartyi* strains. *Philos. Trans. R. Soc., B* **2013**, *368*, 20120321.

(8) Türkowsky, D.; Jehmlich, N.; Diekert, G.; Adrian, L.; von Bergen, M.; Goris, T. An integrative overview of genomic, transcriptomic and proteomix analyses in organohalide respiration research. *FEMS Microbiol. Ecol.* **2018**, *94*, fiy013.

(9) Kublik, A.; Deobald, D.; Hartwig, S.; Schiffmann, C. L.; Andrades, A.; von Bergen, M.; Sawers, R. G.; Adrian, L. Identification of a multi-protein reductive dehalogenase complex in *Dehalococcoides mccartyi* strain CBDB1 suggests a protein-dependent respiratory electron transport chain obviating quinone involvement. *Environ. Microbiol.* **2016**, *18*, 3044−3056.

(10) Hartwig, S.; Dragomirova, N.; Kublik, A.; Türkowsky, D.; von Bergen, M.; Lechner, U.; Adrian, L.; Sawers, R. G. A H_2-oxidizing, 1,2,3-trichlorobenzene-reducing multienzyme complex isolated from the obligately organohalide-respiring bacterium *Dehalococcoides mccartyi* strain CBDB1. *Environ. Microbiol. Rep.* **2017**, *9*, 618−625.

(11) Seidel, K.; Kühne, J.; Adrian, L. The complexome of *Dehalococcoides mccartyi* reveals its organohalide respiration-complex is modular. *Front. Microbiol.* **2018**, *9*, 1130.

(12) Moe, W. M.; Rainey, F. A.; Yan, J. The genus *Dehalogenimonas*. In *Organohalide-Respiring Bacteria*; Adrian, L., Löffler, F. E., Eds.; Springer Berlin Heidelberg: Berlin, 2016; pp 137−151.

(13) Yang, Y.; Higgins, S. A.; Yan, J.; Şimşir, B.; Chourey, K.; Iyer, R.; Hettich, R. L.; Baldwin, B.; Ogles, D. M.; Löffler, F. E. Grape pomace compost harbors organohalide-respiring Dehalogenimonas species with novel reductive dehalogenase genes. *ISME J.* **2017**, *11*, 2767−2780.

(14) Qiao, W.; Luo, F.; Lomheim, L.; Mack, E. E.; Ye, S.; Wu, J.; Edwards, E. A. A dehalogenimonas population respires 1,2,4-trichlorobenzene and dichlorobenzenes. *Environ. Sci. Technol.* **2018**, *52*, 13391−13398.

(15) Siddaramappa, S.; Challacombe, J. F.; Delano, S. F.; Green, L. D.; Daligault, H.; Bruce, D.; Detter, C.; Tapia, R.; Han, S.; Goodwin, L.; Han, J.; Woyke, T.; Pitluck, S.; Pennacchio, L.; Nolan, M.; Land, M.; Chang, Y.-J.; Kyrpides, N. C.; Ovchinnikova, G.; Hauser, L.; Lapidus, A.; Yan, J.; Bowman, K. S.; da Costa, M. S.; Rainey, F. A.; Moe, W. M. Complete genome sequence of *Dehalogenimonas lykanthroporepellens* type strain (BL-DC-9(T)) and comparison to "Dehalococcoides" strains. *Stand. Genomic Sci.* **2012**, *6*, 251−264.

(16) Key, T. A.; Richmond, D. P.; Bowman, K. S.; Cho, Y.-J.; Chun, J.; da Costa, M. S.; Rainey, F. A.; Moe, W. M. Genome sequence of the organohalide-respiring *Dehalogenimonas alkenigignens* type strain (IP3-3T). *Stand. Genomic Sci.* **2016**, *11*, 44.

(17) Molenda, O.; Quaile, A. T.; Edwards, E. A. Dehalogenimonas sp. strain WBC-2 genome and identification of its trans-dichloroethene reductive dehalogenase, TdrA. *Appl. Environ. Microbiol.* **2016**, *82*, 40−50.

(18) Key, T. A.; Bowman, K. S.; Lee, I.; Chun, J.; Albuquerque, L.; da Costa, M. S.; Rainey, F. A.; Moe, W. M. *Dehalogenimonas formicexedens* sp. nov., a chlorinated alkane-respiring bacterium isolated from contaminated groundwater. *Int. J. Syst. Evol. Microbiol.* **2017**, *67*, 1366−1373.

(19) Padilla-Crespo, E.; Yan, J.; Swift, C.; Wagner, D. D.; Chourey, K.; Hettich, R. L.; Ritalahti, K. M.; Löffler, F. E. Identification and environmental distribution of *dcpA*, which encodes the reductive dehalogenase catalyzing the dichloroelimination of 1,2-dichloropropane to propene in organohalide-respiring *Chloroflexi*. *Appl. Environ. Microbiol.* **2014**, *80*, 808−818.

(20) Martín-González, L.; Hatijah Mortan, S.; Rosell, M.; Parladé, E.; Martínez-Alonso, M.; Gaju, N.; Caminal, G.; Adrian, L.; Marco-Urrea, E. Stable carbon isotope fractionation during 1,2-dichloropropane-to-propene transformation by an enrichment culture containing *Dehalogenimonas* strains and a dcpA gene. *Environ. Sci. Technol.* **2015**, *49*, 8666−8674.

(21) Palau, J.; Yu, R.; Hatijah Mortan, S.; Shouakar-Stash, O.; Rosell, M.; Freedman, D. L.; Sbarbati, C.; Fiorenza, S.; Aravena, R.; Marco-Urrea, E.; Elsner, M.; Soler, A.; Hunkeler, D. Distinct dual C−Cl isotope fractionation patterns during anaerobic biodegradation of 1,2-dichloroethane: Potential to characterize microbial degradation in the field. *Environ. Sci. Technol.* **2017**, *51*, 2685−2694.

(22) Palau, J.; Shouakar-Stash, O.; Hatijah Mortan, S.; Yu, R.; Rosell, M.; Marco-Urrea, E.; Freedman, D. L.; Aravena, R.; Soler, A.; Hunkeler, D. Hydrogen isotope fractionation during the biodegradation of 1,2-dichloroethane: Potential for pathway identification using a multi-element (C, Cl, and H) isotope approach. *Environ. Sci. Technol.* **2017**, *51*, 10526−10535.

(23) Mortan, S. H.; Martín-González, L.; Vicent, T.; Caminal, G.; Nijenhuis, I.; Adrian, L.; Marco-Urrea, E. Detoxification of 1,1,2-trichloroethane to ethene in a bioreactor co-culture of *Dehalogenimonas* and *Dehalococcoides mccartyi* strains. *J. Hazard. Mater.* **2017**, *331*, 218−225.

(24) Löffler, F. E.; Sanford, R. A.; Ritalahti, K. M. Enrichment, cultivation, and detection of reductively dechlorinating bacteria. *Methods Enzymol.* **2005**, *397*, 77−111.

https://dx.doi.org/10.1021/acs.jproteome.0c00569
J. Proteome Res. 2021, 20, 613−623

(25) Vallenet, D.; Calteau, A.; Cruveiller, S.; Gachet, M.; Lajus, A.; Josso, A.; Mercier, J.; Renaux, A.; Rollin, J.; Rouy, Z.; Roche, D.; Scarpelli, C.; Médigue, C. MicroScope in 2017: an expanding and evolving integrated resource for community expertise of microbial genomes. *Nucleic Acids Res.* **2017**, *45*, D517−D528.
(26) Armenteros, J. J. A.; Tsirigos, K. D.; Sønderby, C. K.; Petersen, T. N.; Winther, O.; Brunak, S.; von Heijne, G.; Nielsen, H. SignalP 5.0 improves signal peptide predictions using deep neural networks. *Nat. Biotechnol.* **2019**, *37*, 420−423.
(27) Krogh, A.; Larsson, B.; von Heijne, G.; Sonnhammer, E. L. L. Predicting transmembrane protein topology with a hidden markov model: application to complete genomes. *J. Mol. Biol.* **2001**, *305*, 567−580.
(28) Yu, N. Y.; Wagner, J. R.; Laird, M. R.; Melli, G.; Rey, S.; Lo, R.; Dao, P.; Sahinalp, S. C.; Ester, M.; Foster, L. J.; Brinkman, F. S. L. PSORTb 3.0: improved protein subcellular localization prediction with refined localization subcategories and predictive capabilities for all prokaryotes. *Bioinformatics* **2010**, *26*, 1608−1615.
(29) Adrian, L.; Hansen, S. K.; Fung, J. M.; Görisch, H.; Zinder, S. H. Growth of *Dehalococcoides* strains with chlorophenols as electron acceptors. *Environ. Sci. Technol.* **2007**, *41*, 2318−2323.
(30) Nesterenko, M. V.; Tilley, M.; Upton, S. J. A simple modification of Blum's silver stain method allows for 30 minite detection of proteins in polyacrylamide gels. *J. Biochem. Biophys. Methods* **1994**, *28*, 239−242.
(31) Kuntze, K.; Kozell, A.; Richnow, H. H.; Halicz, L.; Nijenhuis, I.; Gelman, F. Dual carbon-bromine stable isotope analysis allows distinguishing transformation pathways of ethylene dibromide. *Environ. Sci. Technol.* **2016**, *50*, 9855−9863.
(32) Parks, D. H.; Imelfort, M.; Skennerton, C. T.; Hugenholtz, P.; Tyson, G. W. CheckM: assessing the quality of microbial genomes recovered from isolates, single cells, and metagenomes. *Genome Res.* **2015**, *25*, 1043−1055.
(33) Price, M. N.; Dehal, P. S.; Arkin, A. P. FastTree: Computing large minimum evolution trees with profiles instead of a distance matrix. *Mol. Biol. Evol.* **2009**, *26*, 1641−1650.
(34) Käll, L.; Krogh, A.; Sonnhammer, E. L. L. Advantages of combined transmembrane topology and signal peptide prediction—the Phobius web server. *Nucleic Acids Res.* **2007**, *35*, W429−W432.
(35) Rahm, B. G.; Morris, R. M.; Richardson, R. E. Temporal expression of respiratory genes in an enrichment culture containing *Dehalococcoides ethenogenes*. *Appl. Environ. Microbiol.* **2006**, *72*, 5486−5491.
(36) Adrian, L.; Rahnenführer, J.; Gobom, J.; Hölscher, T. Identification of a chlorobenzene reductive dehalogenase in *Dehalococcoides* sp strain CBDB1. *Appl. Environ. Microbiol.* **2007**, *73*, 7717−7724.
(37) Payne, K. A. P.; Quezada, C. P.; Fisher, K.; Dunstan, M. S.; Collins, F. A.; Sjuts, H.; Levy, C.; Hay, S.; Rigby, S. E. J.; Leys, D. Reductive dehalogenase structure suggests a mechanism for B_{12}-dependent dehalogenation. *Nature* **2015**, *517*, 513−516.
(38) Atashgahi, S. Discovered by genomics: putative reductive dehalogenases with N-terminus transmembrane helixes. *FEMS Microbiol. Ecol.* **2019**, *95*, fiz048.
(39) Jochum, L. M.; Schreiber, L.; Marshall, I. P. G.; Jorgensen, B. B.; Schramm, A.; Kieldsen, K. U. Single-cell genomics reveals a diverse metabolic potential of uncultivated *Desulfatiglans*-related Deltaproteobacteria widely distributed in marine sediment. *Front. Microbiol.* **2018**, *9*, 2038.

https://dx.doi.org/10.1021/acs.jproteome.0c00569
J. Proteome Res. 2021, 20, 613−623